High Spatial Resolution Imaging of the Contiguous Objects Using Sub-Y-Type Interferometric Synthetic Aperture Radiometer

Ho-Jin Lee, Hyuk Park, Sung-Hyun Kim, Jun-Ho Choi, Seung-Won Seo, and Yong-Hoon Kim
Sensor System Laboratory, Department of Mechatronics,
Gwangju Institute of Science and Technology (GIST)
1 Oryong-dong, Buk-gu, Gwangju 500-712, Korea
TEL:+82-62-970-2412, FAX:+82-62-970-2384, E-mail: ssllhj@gist.ac.kr

Gum-Sil Kang
Satellite Application Department
Korea Aerospace Research Institute
45 Eoeun-dong, Yuseong-gu, Deajeon, 305-333, Korea
E-mail: wimikgs@kari.re.kr

Abstract: Recently the interferometric synthetic aperture radiometer with sub-Y-type antenna array was suggested to improve the spatial resolution than that of conventional Y-type with the same number of antenna elements. The sub-Y-type performance has been reported under a point source target. In this paper, the performance of sub-Y-type is evaluated under contiguous objects. The angular resolution of sub-Y-type with 52 antennas was compared with that of Y-type with the 40 antennas. The images of sub-Y-type and Y-type array were simulated under the contiguous objects. The sub-Y-type showed higher resolution than Y-type in the simulation and experiments. The sub-Y-type has high spatial resolution than Y-type in case of contiguous source as well as single point source.

Keywords: Interferometric Synthetic Aperture Radiometer, Sub-Y-Type Array.

1. Introduction

Interferometric synthetic aperture radiometer was suggested in the 1980s for earth observation at low microwave frequency with an advantage of high resolution [1]. It was proposed as a substitute to real aperture radiometer. It can obtain high resolution images without mechanical scanning. In two-dimensional interferometric synthetic aperture radiometer, an antenna alignment is one of the important design considerations. Because it settles the sampling type of visibility function and the minimum number of visibility samples required for a determined aliasing level. It has been reported that Y-type array with equally spaced antenna is optimal in terms of a narrow beamwidth and wide synthesized field of view [2]. This is applied to develop MIRAS (Microwave Imaging Radiometer by Aperture Synthesis) by the European Space Agency [3]. MIRAS has large Y-type array with 43 antennas per arm spaced 0.89λ (λ: wavelength) at 1.4 GHz in order to obtain 3 dB beamwidth of 0.77°. The requirement for large array to get a high spatial resolution is one of the controversial points, because it causes problems such as complexity and system cost.

A new type of array configuration, the sub-Y-type array is proposed by our research group, SSL(Sensor System Laboratory) at GIST [4][5]. The proposed array type has an improved resolution than the conventional Y-type known as optimal array configuration in the design of 2-D interferometric radiometer.

The 37 GHz interferometric synthetic aperture radiometer with 40 antenna elements is developed to evaluate the performance of sub-Y-type array configuration. The visibility samples for interferometric aperture synthesis are measured by sequentially spacing two antenna elements in required pairs of positions in the near-field condition. Using the reference noise source, the radiometric characteristics of sub-Y-type array configuration were examined. To compare the theoretical results of proposed type, two contiguous noise sources were tested with sub-Y-type and Y-type. The detailed architecture and experimental results are discussed in the following sections.

2. Sub-Y-Type Array Configuration

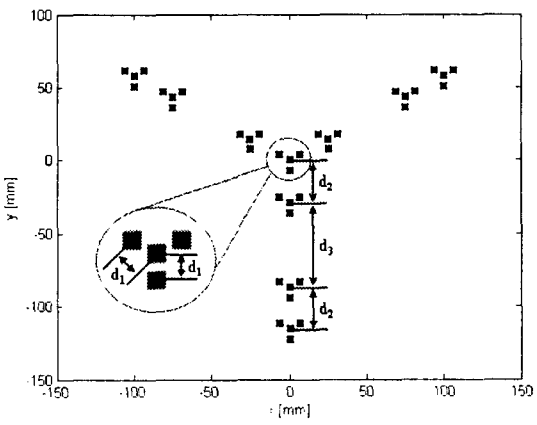

Fig. 1. Sub-Y-type array with 40 antennas.

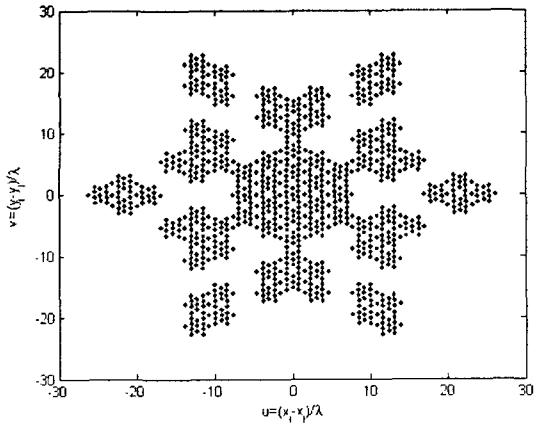

Fig. 2. Visibility samples for sub-Y-type.

In this section the sub-Y-type array configuration is explained. This configuration is suggested to achieve the 2 dimensional high angular resolution images. The antenna array configuration is important because the array type affects the synthesized beam pattern. Several array types have been proposed such as T-, L-, and Y-type. Among these, Y-type array has been proposed as the most efficient configuration that has a large alias free field of view and a narrow synthesized beamwidth compared to other array type under the same number of antenna elements. The sub-Y-type array configuration is devised to obtain wider visibility coverage area than the conventional Y-type array keeping the hexagonal sampling characteristic under the fixed antenna element. Instead it is at the expense of incomplete spatial sampling. The sub-Y-type array configuration is based on sub-array groups where four antenna elements are arranged by d_1 like Y shape. It is based on antenna groups, which consist of two sub-arrays spaced by d_2. The distance d_2 is set to $4d_1$ to obtain a complete sampling on the principle axes, which is required for alias suppression algorithm. The grouping of sub-arrays in Fig. 1 is intended to extent the arm of sub-Y-type array keeping a complete sampling on the principle axes. The spacing between two groups is represented by d_3. The detailed description of sub-Y-type array antenna configuration is presented in [5]. The antenna array configuration of interferometric synthetic aperture radiometer affects on the imaging characteristics because the brightness temperature image is reconstructed from the sampled visibility functions by the inverse Fourier transform. The synthesized beamwidth is inversely proportional to the sample coverage area of visibility functions. The sample coverage is shown in Fig. 2. The visibility samples are not completely samples. However it has the same visibility sample coverage.

3. Simulation

The synthesized beam of the Y-type array and sub-Y-type are simulated under a single point source target and the contiguous targets. For this simulation of Y-type array, 52 antenna elements are used and the distance between the adjacent antennas are equally spaced 0.89λ. To evaluate the performance of the sub-Y-type array, the reconstructed image is simulated using three images. The simulation is performed as follow conditions:

1. Antenna configuration: the Y-type array with 52 antenna elements and the sub-Y-type array with 40 antenna elements are used.
2. Test input images: a single point source target, a single square target and contiguous square targets are used. The distance between the adjacent image sources is to be much smaller that the half-power beamwidth of the PSF.

1) Case I: Single point source target

The first simulation is performed under a single point source target. The object of this is to get the radiometer system response. The system response represents the point spread function (PSF). That is important to analyze the imaging performance of the radiometer because its characteristics such as main beamwidth and sidelobe level are relevant to the imaging performance. In Fig. 3 and Table 1, the beamwidth of Y-type and sub-Y-type are equal. Using less antenna elements, sub-Y-type array achieves the same angular resolution to Y-type array. However the sidelobe of sub-Y-type array is higher than that of Y-type.

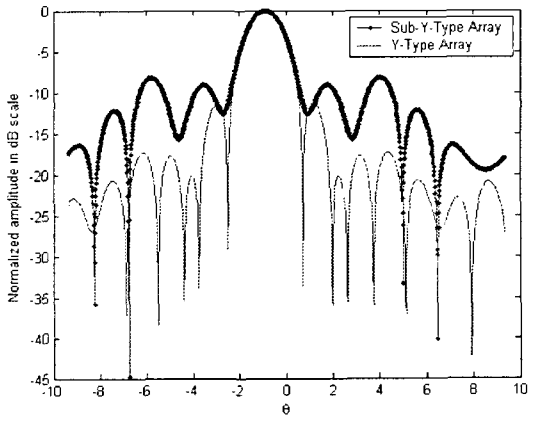

Fig. 3. One dimensional profile.

Table 1. Estimated characteristics of Y-type and sub-Y-type.

	Antenna array type	
	Y-type (52 antennas)	Sub-Y-type (40 antennas)
Beamwidth	1.72°	1.72°
Sidelobe	-11.27 dB	-8.16 dB

2) Case II: Single square target

The next simulation is carried out under a single square target. The results of this are illustrated in Fig. 4. Fig. 4(a) is the real single square target image. The background value in the image is zero. Fig. 4(b) is the reconstructed image using Y-type array. Fig. 4(c) is the reconstructed image using sub-Y-type array. The background value is not zero in Fig. 4(c). There is noise around the

reconstructed image. The edge of the reconstructed image is blurred. The blurred in the background of the image can be reduced using the sidelobe suppression window.

3) Case III: Contiguous square targets

The last simulation is executed under contiguous square target. The results of this are shown in Fig. 5. Fig. 5(a) is the real contiguous multiple square targets image. The background value in the image is zero. Fig. 5(b) is the reconstructed image using Y-type array with 52 antennas. Fig. 5(c) is the reconstructed image using sub-Y-type array with 40 antennas. There are many ghost targets because of the high sidelobe in Fig. 5(c). The sidelobe degrades the reconstructed image. The image is blurred. The ghost signal in the background of the image can be reduced using the sidelobe suppression window.

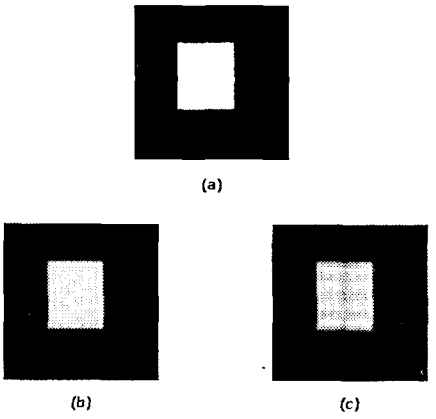

Fig. 4. Simulation of a single square target. (a) Original image. (b) Reconstructed image using Y-type array. (c) Reconstructed Image using sub-Y-type array.

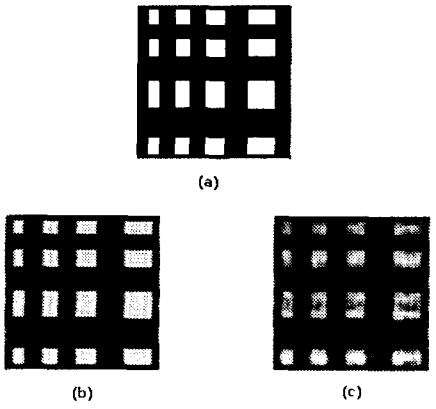

Fig. 5. Simulation of contiguous square targets. (a) Original image. (b) Reconstructed image using Y-type array. (c) Reconstructed image using sub-Y-type array.

Table 2. System Specification and Experiment Environment.

Measurement distance	3.6 m
Center frequency	37 GHz
Correlation bandwidth	100 MHz
Integration time	0.65 μs
Noise bandwidth	96.65 MHz
I/Q demodulator	Software based
Complex correlator	Software based
SNR	30 dB
Receiver gain	80 dB
Channel isolation	> 40 dB
RF image suppression	> 30 dB

4. Experiment Results

37 GHz correlation radiometer was developed to experiment the performance of sub-Y-type array. The system specification and experiment environment are listed in Table 2. The visibility samples are measured by sequentially spacing the two patch antennas in required pairs of positions on the antenna mounting structure. A hot noise source is used as imaging target to evaluate the angular resolution of proposed interferometric synthetic aperture radiometer. This noise point source consists of a matched load, an amplifier, and a 4x4 linear polarization patch antenna. Since the receiving antennas should be in the far field from the target, a measurement range must be more distant than $2L^2/\lambda$ (L=array size). However, the far field condition of a measurement range cannot be satisfied in our indoor experiments. Therefore the phase error has an effect on the synthesized image of the measurements. The sub-Y-type array is designed with 40 channels. The distance of two antennas, d_1 is fixed 0.89λ to compare with Y-type array and also $d_2=4d_1$ and $d_3=8d_1$ are decided to obtain optimum angular resolution [5]. The measured point response of sub-Y-type is affected by phase error because the measurement range is not satisfied with the far field region. In order to keep the same phase error for Y-type and sub-Y-type, the Y-type is constructed with 52 antennas for experiment so that the same visibility coverage of sub-Y-type with 40 antennas is achieved. The point source responses of Y-type array and sub-Y –type antenna configuration are reconstructed from visibility samples of 52 and 40 antennas respectively as shown in Fig. 6. Although the antenna number of sub-Y-type array antenna configuration is reduced by 12 than that of Y-type antenna configuration, but their responses are similar. That is, the angular resolution is improved by 23%. Fig. 6 shows the point source response using the single noise source. The point source is located at the center of the image plane.

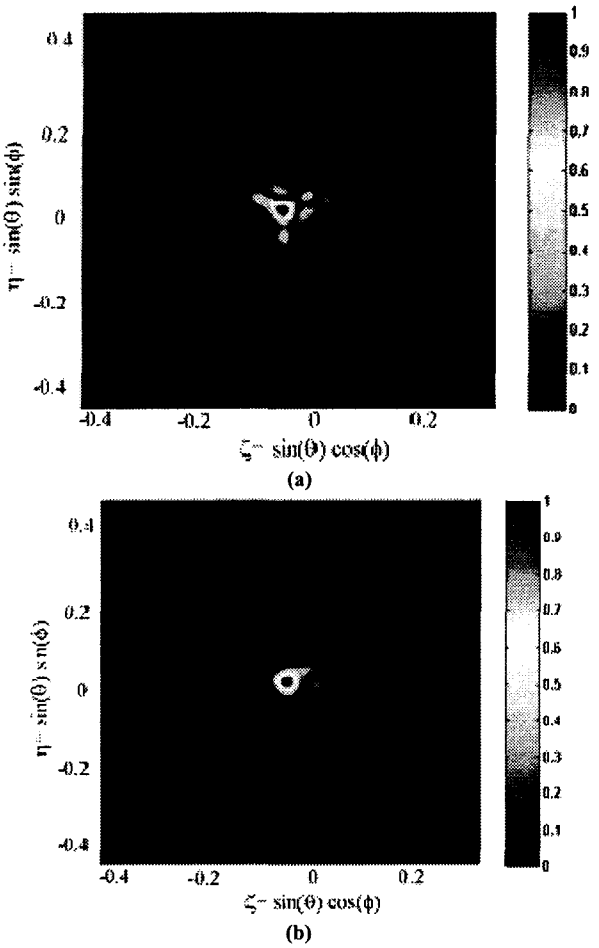

Fig. 6. Response of a noise source. (a) Y-type array. (b) sub-Y-type array.

5. Conclusions

The interferometric synthetic aperture radiometer based on sub-Y-type is developed at 37 GHz. The performance of angular resolution is evaluated by using the point noise source. Using the less antenna elements, the sub-Y-type array achieved the same angular resolution compared with the Y-type array. The performance evaluation shows 23 % improvement of angular resolution than the conventional Y-type in the measurement. It was evaluated. However, sub-Y-type array has a disadvantage that the sidelobe is high. It makes the reconstructed image to be degraded. It needs the additional method to compensate the high sidelobe.

Acknowledgement

This work was supported in part by the Korean Science and Engineering Foundation(KOSEF) through the Advanced Environmental Monitoring Research Center at Gwangju Institute of Science and Technology.

References

[1] C. S. Ruf, C. T. Swift, A. B. Tanner, and D. M. Le Vine, 1988. Interferometric Synthetic Aperture Microwave Radiometry for the Remote Sensing of the Earth, *IEEE Trans. Geosci. Remote Sensing*, 26(5): 597-611

[2] A. Camps, F. Toress, I. Gorbella, J. Bara, and X. Soler, 1997. Calibration and Experimental Results of a Two-Dimensional Interferometric Radiometer Laboratory Prototype, *Radio Science*, 32(5): 1821-1832.

[3] Gumsil Kang, 2004. Study of High Angular Resolution Interferometric Synthetic Aperture Radiometer, Ph. D. dissertation, GIST at Gwangju, Korea.

[4] J. Bara, A. Camps, F. Toress, and I. Corbella, 1998. Angular Resolution of Two-Dimensional, Hexagonally Sampled Interferometric Radiometers, Radio Science, 33(5): 1459-1473.

[5] Yong-Hoon Kim, Gumsil Kang, 2001. Sub-Y-Type Antenna Array Configuration for High Resolution on Application of an Interferometric Synthetic Aperture Radiometer, Specialist Meeting on Microwave Remote Sensing